

This article was downloaded by: [Texas A&M University Libraries]

On: 09 March 2015, At: 11:19

Publisher: Taylor & Francis

Informa Ltd Registered in England and Wales Registered Number: 1072954 Registered office: Mortimer House, 37-41 Mortimer Street, London W1T 3JH, UK



IIE Transactions

Publication details, including instructions for authors and subscription information:
<http://www.tandfonline.com/loi/uiie20>

Modulus prediction of buckypaper based on multi-fidelity analysis involving latent variables

Arash Pourhabib^a, Jianhua Z. Huang^b, Kan Wang^c, Chuck Zhang^c, Ben Wang^c & Yu Ding^d

^a School of Industrial Engineering and Management, Oklahoma State University, Stillwater, OK 74078, USA

^b Department of Statistics, Texas A&M University, College Station, TX 77843-3131, USA

^c H. Milton Stewart School of Industrial and Systems Engineering, Georgia Institute of Technology, Atlanta, GA 30332-0205, USA

^d Department of Industrial and Systems Engineering, Texas A&M University, College Station, TX 77843-3131, USA E-mail:

Accepted author version posted online: 30 Apr 2014. Published online: 05 Nov 2014.



[Click for updates](#)

To cite this article: Arash Pourhabib, Jianhua Z. Huang, Kan Wang, Chuck Zhang, Ben Wang & Yu Ding (2015) Modulus prediction of buckypaper based on multi-fidelity analysis involving latent variables, IIE Transactions, 47:2, 141-152, DOI: [10.1080/0740817X.2014.917777](https://doi.org/10.1080/0740817X.2014.917777)

To link to this article: <http://dx.doi.org/10.1080/0740817X.2014.917777>

PLEASE SCROLL DOWN FOR ARTICLE

Taylor & Francis makes every effort to ensure the accuracy of all the information (the "Content") contained in the publications on our platform. However, Taylor & Francis, our agents, and our licensors make no representations or warranties whatsoever as to the accuracy, completeness, or suitability for any purpose of the Content. Any opinions and views expressed in this publication are the opinions and views of the authors, and are not the views of or endorsed by Taylor & Francis. The accuracy of the Content should not be relied upon and should be independently verified with primary sources of information. Taylor and Francis shall not be liable for any losses, actions, claims, proceedings, demands, costs, expenses, damages, and other liabilities whatsoever or howsoever caused arising directly or indirectly in connection with, in relation to or arising out of the use of the Content.

This article may be used for research, teaching, and private study purposes. Any substantial or systematic reproduction, redistribution, reselling, loan, sub-licensing, systematic supply, or distribution in any form to anyone is expressly forbidden. Terms & Conditions of access and use can be found at <http://www.tandfonline.com/page/terms-and-conditions>

Modulus prediction of buckypaper based on multi-fidelity analysis involving latent variables

ARASH POURHABIB¹, JIANHUA Z. HUANG², KAN WANG³, CHUCK ZHANG³, BEN WANG³
and YU DING^{4,*}

¹*School of Industrial Engineering and Management, Oklahoma State University, Stillwater, OK 74078, USA*

²*Department of Statistics, Texas A&M University, College Station, TX 77843-3131, USA*

³*H. Milton Stewart School of Industrial and Systems Engineering, Georgia Institute of Technology, Atlanta, GA 30332-0205, USA*

⁴*Department of Industrial and Systems Engineering, Texas A&M University, College Station, TX 77843-3131, USA*
E-mail: yuding@iemail.tamu.edu

Received March 2013 and accepted March 2014

Buckypapers are thin sheets produced from Carbon NanoTubes (CNTs) that effectively transfer the exceptional mechanical properties of CNTs to bulk materials. To accomplish a sensible tradeoff between effectiveness and efficiency in predicting the mechanical properties of CNT buckypapers, a multi-fidelity analysis appears necessary, combining costly but high-fidelity physical experiment outputs with affordable but low-fidelity Finite Element Analysis (FEA)-based simulation responses. Unlike the existing multi-fidelity analysis reported in the literature, not all of the input variables in the FEA simulation code are observable in the physical experiments; the unobservable ones are the latent variables in our multi-fidelity analysis. This article presents a formulation for multi-fidelity analysis problems involving latent variables and further develops a solution procedure based on nonlinear optimization. In a broad sense, this latent variable-involved multi-fidelity analysis falls under the category of non-isometric matching problems. The performance of the proposed method is compared with both a single-fidelity analysis and the existing multi-fidelity analysis without considering latent variables, and the superiority of the new method is demonstrated, especially when we perform extrapolation.

Keywords: Buckypaper, carbon nanotubes, latent variables, Gaussian processes, multi-fidelity analysis

1. Introduction

Carbon NanoTubes (CNTs) are a type of carbon structure that is made up of nano-scale tubes (Iijima, 1991). Possessing exceptional thermal and mechanical properties, CNTs are considered to be promising for application to a wide range of products (Tsai *et al.*, 2011). One method to fabricate CNT-based products is through manufacturing thin layers of CNT called buckypaper (Wang *et al.*, 2004). However, the buckypaper itself does not necessarily possess desirable properties for industrial applications (Tsai *et al.*, 2011). One treatment is to add PolyVinyl Alcohol (PVA) to the buckypaper (Zhang *et al.*, 2011), which can produce a high-stiffness product called PVA-treated buckypaper.

Practitioners want to understand how the stiffness of the buckypaper, measured in terms of the Young's modulus, is affected by the addition of PVA in the fabrication process in the presence of other noise variables. A standard approach

is to conduct a set of physical experiments; that is, fabricate a number of buckypapers with varying amounts of the PVA added, measure the Young's modulus of the resulting buckypaper, and fit a functional relationship between the PVA input and the stiffness output. The main problem with this approach is that the physical experiments are expensive to conduct, both time-wise and cost-wise, and measuring the Young's modulus requires a process that damages the buckypaper under test. Realistically, only a small number of such experiments, say, no more than 10 input settings with three to five replications per setting, can be reasonably expected.

In order to complement the physical experiments and expedite product development, a simulation model based on the finite element approximation has been developed to numerically calculate the Young's modulus of the buckypaper under a given amount of PVA additive and a few specifications of CNTs (Wang, 2013). The co-existence of the physical and simulation outputs of the buckypaper fabrication process presents a multi-fidelity analysis problem that has been extensively considered by the academic community (to be reviewed in the following section). In our case, we consider that the physical outputs provide the basic truth

*Corresponding author

Color versions of one or more of the figures in the article can be found online at www.tandfonline.com/uiie.

and are therefore the high-fidelity outputs, whereas the simulation, being an approximation, understandably provides the low-fidelity responses.

In multi-fidelity analysis, one may be provided with data sets created by a physical experiment and a simulation model, such as in the aforementioned buckypaper fabrication process as well as in Kennedy and O'Hagan (2000, 2001), Higdon *et al.* (2004), Reese *et al.* (2004), Bayarri *et al.* (2007), Qian and Wu (2008), Han *et al.* (2009), and Joseph and Melkote (2009), or they can come from two physical processes of different measurement resolutions (Xia *et al.*, 2011) or from two simulation models of different degrees of accuracy (Qian *et al.*, 2006; Xiong *et al.*, 2013). Regardless of the origin of the data, in all of these cases one deals with a situation in which one experiment provides more accurate data (high fidelity) but obtained at a relatively higher cost, and the other experiment, despite being affordable, cannot be relied on solely as the responses or outputs do not reflect the reality very well (low fidelity). Apparently, if one could collect an adequate number of data points from the high-fidelity experiment, we would not need the low-fidelity data. In reality, however, the high cost prohibits practitioners from running the high-fidelity experiments/simulations to obtain a sufficient number of input conditions, as we argued above, and, as a result, the high-fidelity responses, with their inferiority in numbers, cannot be relied on solely either and can only complement, rather than replace, the low-fidelity responses.

Methodologies introduced to tackle the multi-fidelity problems can be classified into two broad categories: (i) methodologies based on building respective models for each of the data sets; and (ii) methodologies that build a model for one of the data sets (low-fidelity ones for example) and then employ a linkage model to connect both data sets.

The methods in the first category hinge upon the idea that the data from each of the corresponding experiments are generated by the same underlying physical mechanism and, therefore, similar models are created for describing the data sets but connected implicitly through the underlying physics. A couple of modeling strategies are reported in the literature. For example, to combine spatial data with different levels of accuracy, Wikle and Berliner (2005) devised a hierarchical Bayesian framework that can be used to make an inference at some predetermined level. Another method was introduced by Reese *et al.* (2004), in which the inference achieved by the data at the low-fidelity level is used as a prior for the model fit using the high-fidelity data.

The methods in the second category assume that the responses in one of the data sets can be reconstructed by including correction terms with the responses in the other data set and using a calibration model to explicitly link the two data sets. So far, the existing methods generally employ a Gaussian Process (GP) to model the low-fidelity experiment and a linear calibration function to connect the two sets of data (see, for example, Kennedy and O'Hagan

(2000, 2001), Higdon *et al.* (2004), Goldstein and Rougier (2006, 2009), Bayarri *et al.* (2007), Qian and Wu (2008), Han *et al.* (2009), Joseph and Melkote (2009), Xiong *et al.* (2009), and Xia *et al.* (2011)).

Irrespective of specific details in each category, they all implicitly assume that the output in each data set is a function of a set of input variables that are the same for both high-fidelity and low-fidelity experiments. More important, those inputs can be directly measured, so that a response from the high-fidelity experiment can be matched with its low-fidelity counterpart. The problem of interest in this article, which is to predict the Young's modulus of PVA-treated buckypaper, appears to present some extra challenges. To illustrate this, let us take a look at Fig. 1, which shows that the simulation model tends to underestimate the Young's modulus for small amounts of PVA and overestimate the modulus for larger amounts of PVA. Understanding of the physical process suggests that such a mismatch in the trend line is caused by the assumption made in the simulation that the effectiveness of PVA—i.e., the amount of the PVA absorbed in the process—stays unchanged as its amount varies. This assumption makes the simulation responses continue to increase at a rapid rate, as the amount of PVA addition increases, whereas the actual physical responses increase slowly or may even level off to a certain degree.

Upon this revelation, our material science collaborators stated that they could modify their simulation code by including an input variable to represent the effectiveness of the PVA. Once this extra variable is used with appropriate input values, the simulation outputs could possibly track the physical responses. The problem, however, is that this PVA effectiveness cannot be directly measured

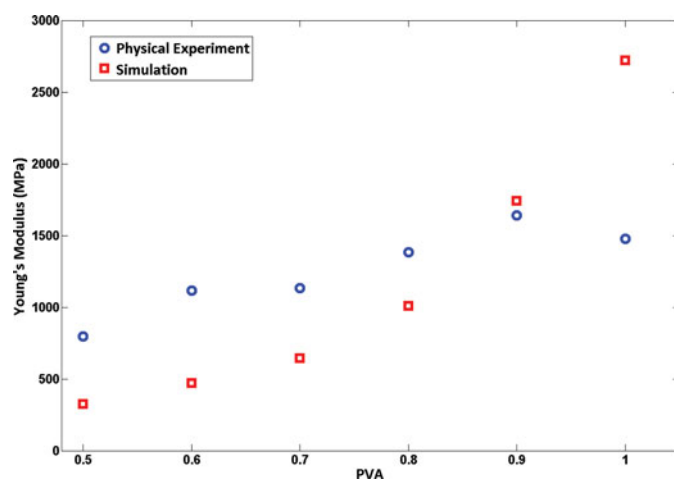


Fig. 1. The Young's moduli of the simulation model and the physical experiment. The x -axis is the weight ratio of PVA additive versus the raw CNTs, both measured in gram. The y -axis is the Young's moduli, with units of milli-pascals. The simulation response increases at a fast rate than the physical response at a high PVA level.

in the physical process and thus becomes difficult to set in the simulation model. In other words, we end up with a multi-fidelity analysis problem with a part of the input variables unobservable in the physical experiment. The unobservable variables have to be represented using latent variables in the corresponding response model. As a result, our problem becomes a multi-fidelity analysis involving latent variables.

We also want to emphasize the difference between latent variables and parameters in the physical experiment. Several multi-fidelity methodologies explicitly consider the existence of some unobserved or uncontrollable features in the physical experiments, generally referred to as calibration parameters (Higdon *et al.*, 2004; Goldstein and Rougier, 2006, 2009; Bayarri *et al.*, 2007; Han *et al.*, 2009; Xiong *et al.*, 2009), however, a calibration parameter is internal to the physical experiments, rather than correlating with inputs to another response. The role of the latent inputs here allows us to link the two experiments, which is a critical aspect in our problem setting us apart from the existing multi-fidelity analyses.

In this article, we introduce a solution approach that targets the specific application as described above. We assume that the latent input variables are correlated with and can be imputed from the observable variables. Our strategy entails the following elements: (i) for the low-fidelity simulation responses, we resort to a GP model; this is the same as in the existing multi-fidelity analyses; (ii) based on the aforementioned assumption, we introduce a functional relationship that connects the latent variables with the observed ones; and (iii) the combined models are formulated as a non-linear optimization problem, which is in turn solved using numerical techniques.

The rest of this article is organized as follows. In Section 2, we formally define the problem and present a mathematical approach. In Section 3, we present our choices of specific model components for the PVA-treated buckypaper fabrication process. In Section 4, we demonstrate that our method outperforms the existing methods in terms of the accuracy of prediction. In particular, the advantage of the proposed method becomes more obvious when it comes to extrapolation. Finally in Section 5, we summarize the article.

2. Latent variable multi-fidelity analysis with correlated inputs

We first introduce the notations and symbols used to define the latent variable multi-fidelity analysis problem in the context of Young's modulus prediction for a PVA-treated buckypaper fabrication process. Consider two data sets available for such a process, the physical experiment denoted by \mathcal{P} and the simulation denoted by \mathcal{S} . We assume that there exists a degree of similarity between the simulation responses and the physical responses so their

integration is justified. The degree of similarity can be easily checked by computing the correlation between the two data sets.

Let $\mathbf{x} \in \mathcal{X}$ be the input vector, then $\mathcal{P} = \{(\mathbf{x}, P(\mathbf{x})) : \mathbf{x} \in \mathcal{X}\}$ where $(\mathbf{x}, P(\mathbf{x}))$ is an input–output pair for the physical experiment. Similarly, we have $\mathcal{S} = \{(\mathbf{x}, S(\mathbf{x})) : \mathbf{x} \in \mathcal{X}\}$ where $(\mathbf{x}, S(\mathbf{x}))$ is an input–output pair for the simulation. Assume we can decompose the components of the vector \mathbf{x} into two parts such that $\mathbf{x} = (\mathbf{x}^o, \mathbf{x}^m)$, where the subscripts o and m stand for “observable” and “missing,” respectively. Then, we can express the functional relation between inputs and outputs in the two experiments as $P = P(\mathbf{x}^o, \mathbf{x}^m)$ and $S = S(\mathbf{x}^o, \mathbf{x}^m)$. In other words, both physical experiment and simulation are functions of $\mathbf{x} = (\mathbf{x}^o, \mathbf{x}^m)$. In the physical experiment, however, only a subset of components of the input—i.e., \mathbf{x}^o —can be specified, whereas in the simulation, both \mathbf{x}^o and \mathbf{x}^m can be specified.

In order to handle the latent variables, we believe that their values need to be in some way determined by those of the observable inputs in \mathbf{x}^o , because if \mathbf{x}^m s are completely uncorrelated to anything we can observe, it becomes impossible to make an inference about them. Based on this understanding, we assume that \mathbf{x}^m s can be described by using the observations in \mathbf{x}^o , through a relationship $g(\cdot)$ and subject to a prescribed level of discrepancy. Specifically, we intend to find the relationship $g(\cdot)$ by minimizing the difference between the simulation outputs and the physical experiment outputs; that is,

$$\begin{aligned} & \min_{g \in \mathcal{G}} \mathcal{L}(P(\mathbf{x}^o, \mathbf{x}^m), S(\mathbf{x}^o, \mathbf{x}^m)), \\ & \text{s.t.} \quad \int_{\mathcal{X}} [\mathbf{x}^m - g(\mathbf{x}^o)]^2 \mu(d\mathbf{x}) \leq \delta, \quad g \in \mathcal{G}, \quad (1) \end{aligned}$$

where $\mathcal{L}(\cdot, \cdot)$ is a loss function, \mathcal{G} is a class of functions to which g is deemed to belong, and δ is the predetermined discrepancy allowance in terms of some metric induced by a measure $\mu(\cdot)$. The integral constraint connects the unobservable variables \mathbf{x}^m with the observed variables \mathbf{x}^o , by minimizing the average difference between the latent variables and the fitted values based on the estimated relationship.

This formulation is in general difficult to solve. To make it tractable, we would like to introduce a few simplifications. Since we care about the mean prediction, the loss function $\mathcal{L}(\cdot, \cdot)$ is chosen to be a squared error loss function. An alternative choice is the absolute error loss, and its use leads to optimality in median estimation. The absolute error loss is more robust to the existence of outliers, whereas the squared error loss is easier to optimize. In our application, the outlier problem is not a source of concern, so we choose to use the squared error loss.

Being multi-fidelity means that the simulation responses generally differ from the physical responses by a noticeable bias. Without bias, people could simply run the low-fidelity simulation a large number of times and average the responses to produce a result comparable to the high-fidelity

source. In reality, the low-fidelity data sources are inherently inferior because the bias cannot be reduced or eliminated through averaging. When using the squared error loss function, we would like to include a bias term $B(\mathbf{x}^o, \mathbf{x}^m)$, the value of which may depend on the input conditions in general. Under this general circumstance, we assume that $B(\mathbf{x}^o, \mathbf{x}^m)$ can be parameterized by a set of parameters Θ_B . One example of such parameterization is to use a GP to model the bias $B(\mathbf{x}^o, \mathbf{x}^m)$ as a function of the input conditions; as such, Θ_B contains the parameters in the GP model.

The loss function will be evaluated using a set of training data. Suppose that we execute n runs of high-fidelity experiments, having as their input conditions as $\mathbf{x}_1^o, \mathbf{x}_2^o, \dots, \mathbf{x}_n^o$, and the i th experiment is replicated n_i times. Then, the noise contaminated responses of the high-fidelity experiments are

$$y_{ij} = P(\mathbf{x}_i^o) + \epsilon_{ij}, \quad i = 1, 2, \dots, n, \text{ and } j = 1, \dots, n_i, \quad (2)$$

where $\epsilon_{ij} \sim \mathcal{N}(0, \sigma^2)$ captures variability in y due to both measurement errors and uncertainty associated with unknown latent variable \mathbf{x}_i^m .

In parallel, we also execute a set of low-fidelity simulations. Here we are primarily concerned with the so-called *deterministic simulations* that yield the same response when run repeatedly under the same input condition. The deterministic simulations are usually referred to as computer experiments (Santner *et al.*, 2003). The simulation, being low cost computationally, can be run a large number of times. Suppose there are a total of $N (>> n)$ runs for the observable variables and L runs for the unobserved variables (recall that both of the variables can be specified in the computer experiment), then

$$S_{i\ell} = S(\mathbf{x}_i^o, \mathbf{x}_i^m), \quad i = 1, 2, \dots, N, \text{ and } \ell = 1, \dots, L. \quad (3)$$

Understandably, when planning for the two sets of experiments, we would like the input conditions used in the physical experiment to be a subset of those used in the computer experiment.

The simulation code has to be run at specific values of the input variables, so that including the simulation directly in an optimization formulation creates a continuous-discrete mixed optimization problem that is usually harder to solve. To alleviate this problem, we use a Gaussian process to model the simulation responses $\{S_{i\ell}\}$ and denote the resulting GP model as $\widehat{S}(\mathbf{x}^o, \mathbf{x}^m)$. The GP model provides a smooth and continuous response over the design space, and using the GP model in the objective function makes the problem easier. We want to note that modeling the low-fidelity response using GP models is a standard practice in the existing multi-fidelity analysis literature (for example, Kennedy and O'Hagan (2000, 2001); Qian and Wu (2008); Xia *et al.* (2011), among others) but the motivation of doing so here is slightly different.

We believe that the choice of \mathcal{G} will have to be decided according to specific applications. Generally the governing physics of a process should indicate whether \mathbf{x}^o and \mathbf{x}^m are related and, if so, how. Here we assume that the class of \mathcal{G} can be parameterized through a set of parameters in $\Theta_{\mathcal{G}}$.

Provided all of the above simplifications and specifications and, moreover, choosing a counting measure for μ , the original optimization formulation can be rewritten, for a given δ , as

$$\min_{\Theta_B, \Theta_{\mathcal{G}}} \sum_i \sum_j (y_{ij} - \widehat{S}(\mathbf{x}_i^o, \mathbf{x}_i^m) - B(\mathbf{x}_i^o, \mathbf{x}_i^m; \Theta_B))^2, \quad (4)$$

$$\text{s.t.} \quad \sum_{i=1}^n |\mathbf{x}_i^m - g(\mathbf{x}_i^o; \Theta_{\mathcal{G}})|^2 \leq \delta, \quad (5)$$

where the parameters of the bias and the linkage function g are explicitly mentioned to demonstrate how the decision variables impact the optimization problem. However, for simplicity of notation, hereafter we drop the explicit notational dependencies, namely, using $B(\mathbf{x}_i^o, \mathbf{x}_i^m)$ for $B(\mathbf{x}_i^o, \mathbf{x}_i^m; \Theta_B)$ and $g(\mathbf{x}_i^o)$ for $g(\mathbf{x}_i^o; \Theta_{\mathcal{G}})$.

Solving the optimization problem (4)–(5) requires imposing additional constraints on the relation between observed and latent variables. This is due to the fact that we cannot observe \mathbf{x}_i^m and we need to impute those values in the optimization procedure. Therefore, depending on the nature of the application, one needs to make pertinent assumptions to solve problems (4)–(5). For example, if the particular application permits and g is selected to be flexible enough, one may assume $\delta = 0$, which in essence implies \mathbf{x}_i^m can be imputed by $g(\mathbf{x}_i^o)$. In Section 3 we proceed by considering a similar approach and demonstrate how one can utilize such a dependency toward devising a tractable optimization problem for buckypaper fabrication. In Section 3.3, we choose the appropriate g function, and in Section 3.4 we present additional regulations to be used for the buckypaper fabrication process and finally solve the above optimization problem.

3. PVA-treated buckypaper fabrication process model

In this section, we specify the model components for the PVA-treated buckypaper fabrication process. In this application, \mathbf{x}^o represents the PVA amount, denoted as p and measured by the weight ratio of the PVA additive versus the raw carbon nanotubes (see also the x -axis of Fig. 1), and \mathbf{x}^m is the absorption rate of the PVA; i.e., the effectiveness of the PVA, denoted as α and expressed in percentage, so that $0 \leq \alpha \leq 1$.

3.1. Design of experiments

Since \mathbf{x}^o is one dimensional, the design of physical experiments is straightforward. Our material scientist partners set the PVA amount range to be between 0.4 and

1.2 and conducted a total of $n = 17$ physical experiments with p_i s evenly spread over the input range. Under each p_i level, there were five replications, namely, $n_i = 5$ for all $i = 1, \dots, n$. There were therefore a total of 85 physical experiments conducted. We want to note that in this study, the number of physical experiments is relatively large because we need extra data for the validation purpose. In practice, it is usually difficult to afford this level of data amount.

The simulation code takes two inputs p and α . The simulation code does involve a group of randomly generated parameters associated with CNTs, such as a CNT diameter, length, and orientation, so its response is not entirely deterministic. However, the simulation code generates a large number of CNTs to mimic the underlying structure in a buckypaper, and the resulting Young's modulus is mostly affected by the two inputs mentioned above. The randomness of the response, under a given setting of p , is much smaller compared with the randomness in the physical experiments. Thus, we believe that the simulation can be reasonably approximated by a deterministic computer experiment.

The computer experiment was designed to cover the PVA amount in the range $0.5 \leq p \leq 1$. The physical responses outside this range were reserved to validate the quality of the extrapolation. The simulation code we use has a restriction on the product of $p \times \alpha$. This product indicates the effective PVA level and cannot be smaller than 0.40 in the simulation code (Wang, 2013); otherwise, the simulation returns a Young's modulus value that is virtually zero. This is one of the limitations of the current simulation code for the computer experiments that the material scientists are working on to improve. Given this restriction, our design input space for the computer experiment is no longer a rectangular region.

This type of design problems is generally solved through a space-filling design formulation (Johnson *et al.*, 1990). The basic idea is to find the design points that minimize the maximum inter-point distance; this is the so-called minimax design criterion. Alternatively, a maximin criterion can be used as well (Stinstra *et al.*, 2003). Suppose we choose the minimax criterion. The design problem can be expressed as follows: for a fixed number of design points n_s , find a set of design points $D \subset T$ that solves the following optimization formulation:

$$\inf_D \sup_{t \in T} \rho(t, D) \quad (6)$$

s.t. $|D| = n_s, \quad D \subset T,$

where $\rho(t, D) = \inf_{d \in D} \rho(t, d)$ is the inter-point distance, $|D|$ denotes the cardinality of the set D , and T is the feasible region from which a candidate design point is chosen. Specifying T differentiates the non-regular designs of arbitrary shape from the regular designs of a rectangular design region. When T is a bounded polytope, Draguljć *et al.* (2010) developed an efficient algorithm that finds the optimal design. The feasibility constraint for a polytope T

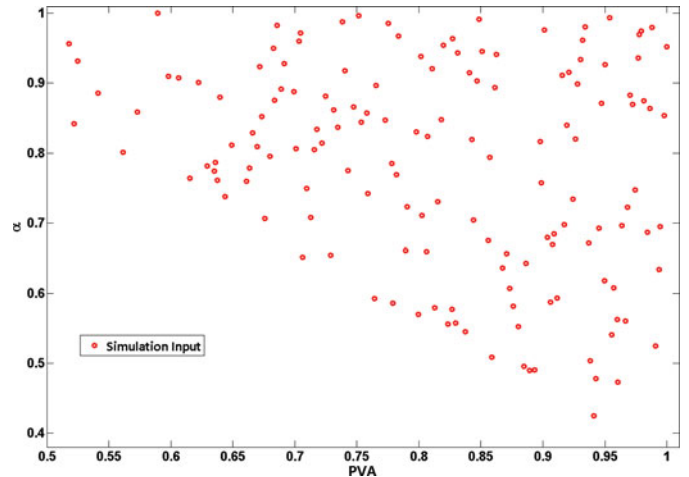


Fig. 2. The design layout for the computer experiment.

is specified as

$$\begin{aligned} \mathbf{A}t &\leq \mathbf{r}, \\ \mathbf{l} &\leq \mathbf{t} \leq \mathbf{u}, \end{aligned} \quad (7)$$

for some matrix \mathbf{A} and vectors \mathbf{r} , \mathbf{l} , and \mathbf{u} , where the inequality should hold point-wise between the corresponding vectors. Using this set of constraints, together with the minimax design criterion, Draguljć *et al.* (2012) showed that it can be solved using a sequential algorithm entailing mainly linear operations. For other alternatives regarding space-filling designs—for example, sliced Latin hypercube designs—readers may refer to Qian and Wu (2009) and Qian (2012).

The design area of our computer experiments can be duly represented by a polytope. Specifically, let $\mathbf{t} = (p, \alpha)^T$, then the design space can be represented in terms of Equation (7) using the following values:

$$\begin{aligned} \mathbf{A} &= [-0.8, -1], & \mathbf{r} &= -1.2, \\ \mathbf{l} &= [0.5, 0.4]^T, & \mathbf{u} &= [1, 1]^T. \end{aligned}$$

Note that as only one of the constraints is non-parallel to an axis, the matrix \mathbf{A} degenerates to a 1×2 vector and \mathbf{r} to a real number. The number of points n_s (i.e., $|D| = n_s$) is decided such that the subsequent surrogate GP model for the low-fidelity data suitably represents the corresponding response surface. Using a few rounds of trial and error, we settled at $n_s = 150$. Note that the number of low-fidelity input settings is about one order of magnitude higher than that of the high-fidelity physical experiment (150 versus 17). Figure 2 displays the selected design points for (p, α) in this computer experiment.

3.2. Gaussian process model and bias term

Once the experimental designs are finished and data are collected, we are ready to train a GP model for the

low-fidelity responses and, if needed, for the bias correction term.

The key aspect in training a GP model is to specify a covariance function, which, loosely speaking, determines the similarity of the response surface at different locations. Here we chose a Squared Exponential (SE) covariance function; that is,

$$K_{SE}(\mathbf{x}_i, \mathbf{x}_j) = \sigma_f^2 \exp\left(-\frac{\|\mathbf{x}_i - \mathbf{x}_j\|^2}{2\eta}\right), \quad (8)$$

where σ_f^2 and η are the variance parameter and scale parameter, respectively, in the covariance function, and they are estimated using the low-fidelity data obtained in the previous subsection. Here we omit the detailed procedure of fitting a GP model; interested readers can find well-established algorithms in Rasmussen and Williams (2006).

The SE covariance function is arguably the most widely used form in many applications and it is isotropic. We did try the so-called automatic relevance determination version of the SE covariance function that uses different scale parameters for each dimension. The fitted GP models using both choices did not differ significantly. We chose the SE covariance function for its simplicity.

Concerning the choice of the bias term, we believe that it is adequate to use a constant in this buckypaper fabrication process because the resulting response surface is not complicated. Making the bias term more flexible does not create much added value. Given this choice, the parameter $\Theta_B = \{B\}$.

3.3. Choice of the g function

Based on our understanding of the physical process, the absorption rate of the PVA appears to be in a monotonically decreasing relation with the PVA amount (Zhang *et al.*, 2011). This implies that when $\mathbf{x}^o = 0.7$, the corresponding absorption rate = 75%, and when $\mathbf{x}^o = 0.8$, the corresponding absorption rate is smaller than 75%. This intuitively explains why the physical responses do not increase with a rapid rate as in the simulation responses in which the absorption rate is set constant for all PVA levels. For this reason we chose \mathcal{G} as the class of smooth monotonically decreasing functions.

For the PVA-treated buckypaper fabrication process, we model function $g(\cdot)$ as a sum of monotone splines. Specifically,

$$g = \sum_{q=1}^Q g_q, \quad (9)$$

$\log(-Dg_q)$ is differentiable and

$$D\{\log(-Dg_q)\} = \frac{D^2 g_q}{Dg_q} \quad (10)$$

is Lebesgue square integrable, where D^m represents taking the derivative of order $m > 0$. These conditions guarantee that g_i is smooth and strictly monotonically decreasing (Ramsay, 1998). For different choices of q , $g(\cdot)$ can take a variety of forms which results in a rich and flexible set of functions.

In the buckypaper fabrication process, since the observable and unobservable variables both have a single element, the function form of $g(\cdot)$ can be greatly simplified. In a one-dimensional space, one solution to differential equation (10) is $g_q(p) = a^{b \times p}$, provided that $a \times b < 0$, thereby assuming $Q = 1$, $g(p) = a^{b \times p}$ is an option for the linkage function. This simple form is desirable as it facilitates the subsequent optimization problem for linking the two experiments without sacrificing the flexibility of the model. We report the results of numerical analysis in Section 4, and we compare this simple choice of g function with a few other alternatives and show that this choice suits our problem well. Given this choice, the function $g(\cdot)$ can be parametrized by $\Theta_g = \{a, b\}$.

3.4. Solution approach

The final step is to solve optimization (4)–(5). Based on our understanding of the buckypaper fabrication process, we believe it is reasonable to assume that the relation between the latent variables can be expressed as a nonlinear function of the observed variables plus a residual difference, such that

$$\mathbf{x}^m = g(\mathbf{x}^o) + e, \quad (11)$$

where $e \sim \mathcal{N}(0, \tilde{\sigma}^2)$. Then, in order to solve optimization (4)–(5), we can simply replace the unknown latent variables \mathbf{x}_i^m with its sample mean, $g(\mathbf{x}_i^o)$, for $i = 1, 2, \dots, n$, and plug the sample mean into the optimization formulation. When taking this approach, we can express the optimization problem as

$$\min_{\Theta_B, \Theta_g} \sum_i (\bar{y}_i - \widehat{S}(\mathbf{x}_i^o, g(\mathbf{x}_i^o)) - B(\mathbf{x}_i^o, g(\mathbf{x}_i^o)))^2, \quad (12)$$

where $\bar{y}_i = 1/n_i \sum_{j=1}^{n_i} y_{ij}$. The resulting optimization problem can be solved by standard nonlinear optimization techniques.

On solving the above optimization problem (12), the multi-fidelity analysis yields a linkage function $g(\cdot)$, determined by \hat{a} and \hat{b} (estimated parameters in Θ_g), and a bias function $B(\mathbf{x}_i^o, \mathbf{x}_i^m)$, determined by \hat{B} (estimated parameter in Θ_B). For any given test case that has an observable \mathbf{x}_*^o , the linkage function $g(\cdot)$ would determine an associated unobservable input component \mathbf{x}_*^m that represents the average value of the unobserved latent variables for the input \mathbf{x}_*^o . With both \mathbf{x}_*^o and \mathbf{x}_*^m , the corresponding low-fidelity simulation response (or its GP surrogate model response) as well as the bias correction can be computed. Adding the low-fidelity simulation response (or its GP model response) and the bias correction together

produces a multi-fidelity prediction for the input \mathbf{x}_*^o . Specifically, given \mathbf{x}_*^o , we have $\mathbf{x}_*^m = g(\mathbf{x}_*^o)$ and the predicted value $y_* = \widehat{S}(\mathbf{x}_*^o, \mathbf{x}_*^m) + B(\mathbf{x}_*^o, \mathbf{x}_*^m)$. Furthermore, as the optimization yields the functional relationship $g(\cdot)$, one can utilize that information for a better understanding of the process. Indeed, understanding how the latent and observed variables connect can provide insight into the physical process. This fact could be of significant importance for engineers who design or operate the application process.

Using the notations and specific models presented in Sections 3.1, 3.2, and 3.3, we can further simplify the optimization problem (12) as

$$\begin{aligned} \min_{\theta \in \Theta} u(\theta) &= \sum_{i=1}^n (\bar{y}_i - \widehat{S}(p_i, g(p_i)) - B)^2, \\ \text{s.t. } \Theta &= \{(a, b, B) \in \mathbb{R}^3 \mid a \times b < 0\}, \end{aligned} \quad (13)$$

where Θ is used to collect the parameters in both Θ_B and Θ_G .

We solve this constrained optimization problem (13) numerically using a steepest descent algorithm. We sequentially update the parameter values by moving opposite the gradient direction for each parameter. The steps for this procedure are summarized in Algorithm 1. The parameter ω^* in the algorithm determines the length of each optimization step. Specifically, to find the value of ω^* at each step, we discretize the interval $(0, 1)$ and choose a value that provides the largest decrease in the objective function:

$$\omega^* = \arg \min_{\omega \in (0,1)} u(\theta_\ell^\omega) \quad \text{for } \ell = 1, 2, 3, \quad (14)$$

where θ_ℓ is the ℓ th parameter in Θ . Here we have three θ parameters, namely, $\theta_1 = a$, $\theta_2 = b$, and $\theta_3 = B$. In the above expression, $\theta_\ell^\omega = \theta_\ell - \omega \partial u(\theta) / \partial \theta_\ell$ and $u(\theta)$ is defined in Equation (13). The derivatives of $\widehat{S}(p_i, g(p_i))$ with respect to a and b are computed numerically. Also, to ensure the relation $a \cdot b < 0$ holds, the step to update b is performed only if the resulting b has a different sign from the current value for a . As the value of objective function decreases at each stage, the algorithm continues until the change in the objective function is negligible, with the algorithm determining that location as a local optimum. The parameters of the covariance function (8) for the GP remain unchanged as the algorithm proceeds, because those values were estimated solely using the low-fidelity data prior to the iterations of the algorithm.

In fact, our multi-fidelity analysis problem can be seen as a special case of matching a one-dimensional (1D) curve to a two-dimensional (2D) surface in the three-dimensional Euclidean space. Here the Euclidean space is generated by (p, α) together with the Young's modulus, whereas the 2D surface is the response surface generated by the simulation model and the 1D curve is formed by the responses of the physical experiment. Once the 2D surface is constructed, one can choose to position the 1D curve such that the response values associated with different locations (i.e., PVA

Algorithm 1 Sequential Update for Optimization Problem (13)

- 1: Set $\theta = (1, -0.1, 500)$
 - 2: **repeat**
 - 3: Calculate ω^* according to Equation (14)
 - 4: $a \leftarrow a + 2\omega^* \sum_{i=1}^n \{(\bar{y}_i - \widehat{S}(p_i, g(p_i)) - B) \frac{\partial}{\partial a} \widehat{S}(p_i, g(p_i))\}$
 - 5: $b \leftarrow b + 2\omega^* \sum_{i=1}^n \{(\bar{y}_i - \widehat{S}(p_i, g(p_i)) - B) \frac{\partial}{\partial b} \widehat{S}(p_i, g(p_i))\}$
 - 6: $B \leftarrow B + 2\omega^* \sum_{i=1}^n (\bar{y}_i - \widehat{S}(p_i, g(p_i)) - B)$
 - 7: Re-evaluate $\widehat{S}(p_i, g(p_i))$ based on (a, b)
 - 8: $\theta \leftarrow (a, b, B)$
 - 9: **until** Local minima are found
 - 10: $\widehat{\theta} \leftarrow \theta$
-

levels) on the curve can be matched to those on the 2D surface as close as possible, after a bias adjustment. Once such a match is found, it reveals the linkage function between the two variables, as illustrated in Fig. 3. In our solution procedure, the manipulation of the position of the 1D curve is in fact done through specifying and solving for the linkage function, as we presented in the preceding sections.

4. Results

In this section, we evaluate the performance of the proposed multi-fidelity analysis method. In the first subsection, we compare the performance of the proposed method with two alternatives, and in the two following subsections we investigate the impact of the amount of high-fidelity data on the multi-fidelity analysis and the effect of different choices of the linkage function.

4.1. Performance comparison

Concerning the multi-fidelity analysis problem involving latent variables, we note two alternatives to what is presented in this article.

1. Since the effectiveness of PVA is not observable, one may argue that we should simply ignore its existence and use whatever is observable to conduct a multi-fidelity analysis following the procedure, say, in Kennedy and O'Hagan (2001) or in Reese *et al.* (2004).
2. Because the response of the low-fidelity computer experiment, while using the observable variable alone (i.e., the PVA amount), could possibly mislead us, it may be appropriate to rely solely on the data of the physical experiment to make predictions at an input level where experimental data are not available. To do this, a GP model can be used to fit the physical data and make predictions. We refer to option (1) as the Multi-Fidelity Analysis without considering the latent variables ("MFA w/o LA"),

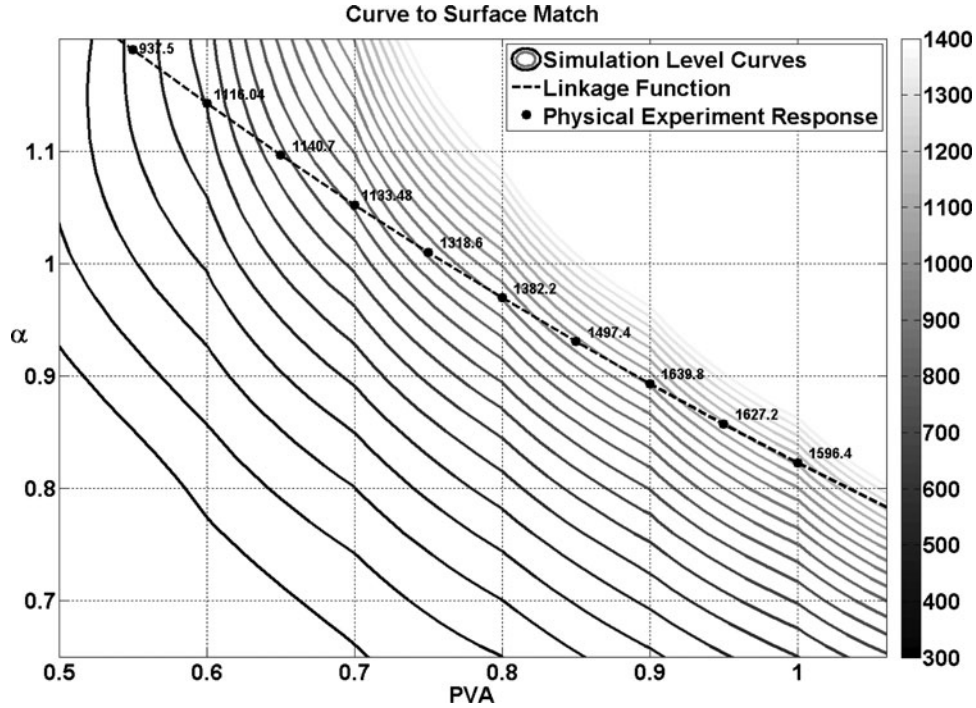


Fig. 3. The curves are the level sets for the simulation surface with step size of 50. The sidebar represents the Young's modulus from the simulation model, where smaller values are represented by darker colors. The dashed curve shows the linkage function. The values close to the dark circles are the Young's modulus from the physical experiment given the corresponding PVA values. The linkage function is decided such that the overall difference between the physical experiment responses and the simulation responses, plus some constant bias, is minimized.

option (2) as a Single-Fidelity Analysis (SFA), and our proposed method as “MFA with LA.”

More specifically, in MFA w/o LA, we assume that the physical experiment value for run i (i.e., $P(p_i)$) could be modeled after a bias and scale change on the simulation response $\widehat{S}(p_i)$. Here, $\widehat{S}(p_i)$ is the average of the surrogate model $\widehat{S}(p_i, \alpha)$ over all possible values of α . The calibration model can be expressed as

$$P(p_i) = \beta_0 + \beta_1 \widehat{S}(p_i) + \gamma_i, \quad (15)$$

where β_0 and β_1 are constants and $\gamma_i \sim \mathcal{N}(0, \sigma_\gamma^2)$. Then the model can be readily solved following the procedure in Kennedy and O'Hagan (2001).

On the other hand, when choosing option (2)—i.e., SFA—we simply train a one-dimensional GP using the training data $\{(p_i, y_{ij}), i = 1, 2, \dots, n; j = 1, 2, \dots, n_i\}$.

To evaluate the performance of a method, we divide the physical experiment data into the training set and test set: use the training set to fit a model during the analysis step and use the test set to compute a performance measure. Note that the low-fidelity data are only used in the training (model fitting) stage not in the testing stage, because the outcome from a MFA is supposed to be better than the low-fidelity response; otherwise, it is of no value to conduct the MFA. One performance measure we use is the Standardized

Root Mean Squared Error (SRMSE):

$$\text{SRMSE} = \sqrt{\frac{\sum_{i=1}^{n_i} [(\hat{y}_i - \bar{y}_i) / \bar{y}_i]^2}{n_i}}, \quad (16)$$

where \hat{y}_i denotes the predicted value (i.e., a method's output) when given the i th observable input \mathbf{x}_i^q in the test set and n_i is the number of data points in the test set. In addition, as suggested by a reviewer, we consider the Standardized Maximum Absolute Deviation.

$$\text{SMAD} = \max \{(\hat{y}_i - \bar{y}_i) / \bar{y}_i\}; \quad i = 1, \dots, n_i. \quad (17)$$

Depending on how the training/test data sets are generated, we produce the following three types of performance measures:

1. Leave-One-Out (LOO): For the details of LOO cross-validation, please refer to Hastie *et al.* (2001). The reported LOO SRMSE is the average of 13 SRMSEs computed when one of the physical data points was left out during the training stage for the physical data in the range of $0.5 \leq p \leq 1.1$ (therefore $n = 12$ for each case).
2. Extrapolation (EXT): Under this circumstance, the training data set contains all of the physical data in the range of $0.5 \leq p \leq 1.1$. Four pairs of data points

Table 1. Comparison of methods: the two rightmost columns show the improvement percentage of the proposed method over the other two methods

	SRMSE			Improvement (%)	
	MFA with LA	SFA	MFA w/o LA	over SFA	over MFA w/o LA
LOO	0.0032	0.0045	0.0140	29	77
EXT	0.0392	0.0806	0.1501	51	73
INT	0.0383	0.0547	0.0681	30	43
	SMAD			Improvement (%)	
	MFA with LA	SFA	MFA w/o LA	over SFA	over MFA w/o LA
LOO	0.0092	0.0097	0.0195	5	20
EXT	0.0885	0.0993	0.1666	11	47
INT	0.0612	0.0818	0.0923	25	34

outside this range, two with $p < 0.5$ and two with $p > 1.1$, were used as the test set (therefore $n = 13$).

- Interpolation (INT): Under this circumstance, we select eight of the physical data points, evenly spread over the input region, as the training set and use the remaining as the test set (therefore, $n = 8$).

Table 1 shows a comparison of results from the three different methods, where the numbers in the “Improvement” column are the reduction of SRMSE or SMAD, expressed as a percentage, when the proposed MFA method is compared with the other two methods. As evident in the table, the proposed method outperforms the other two algorithms for all evaluation measures. When the latent variable is present, and thus the low-fidelity response deviates significantly from the high-fidelity response over certain areas of the input space, the existing multi-fidelity analysis (“MFA w/o LA”) performs even worse than the SFA. This outcome suggests that without a new methodology to handle the latent variables, we would be better off by ignoring the low-fidelity responses.

It is interesting to note that the proposed MFA performs much better than the SFA and MFA w/o LA when they are used for extrapolation. Extrapolation is considered more valuable for product development and process control purposes because a good extrapolation tool can save time and cost while exploring a large response surface. It is a common understanding that SFA does not have a good extrapolation ability since it is purely data-driven. The MFA is supposed to improve SFA’s extrapolation ability, because the low-fidelity model is supposed to be still physics-based and can guide its response when performing extrapolation. Of course, this is only true when the low-fidelity model uses the right physics to guide its response. We believe this is one critical reason why it is important to understand the role of the latent variables and then incorporate them into the MFA.

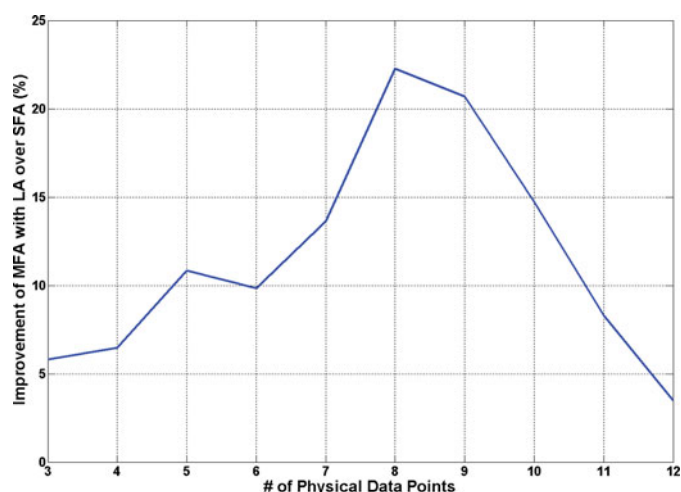
4.2. Impact of the amount of high-fidelity data

We are interested in knowing how the amount of high-fidelity data impacts the quality of the MFA. Here our

benchmark is the SFA, since the previous subsection establishes that with the presence of latent variables the SFA outperforms the MFA that does not consider the latent variables.

To this end, we selected a subset of data points from the physical experiment and conducted both SFA and MFA (with LA) using the same set of data. We kept the same number of replications per input level as before but chose a subset of the amount PVA. We started with four PVA levels, which were randomly selected, as the training data, and then we added one extra PVA level at a time and observed the difference between the SRMSEs when using the two methods; the SRMSEs were obtained by comparing the predicted values at the PVA levels not used in the training data with their counterparts from the physical experiment.

Figure 4 displays the results. If we look at the right-hand side of the figure when there is a large amount of high-fidelity physical data, there is not much difference between SFA and MFA. This is expected, as we previously argued, with a sufficient amount of high-fidelity data SFA can do

**Fig. 4.** Improvement of MFA with LA over SFA as a function of the number of high-fidelity data points.

an adequate job of making predictions and, consequently, the low-fidelity data may no longer be needed. As we move along the horizontal axis to the left and the amount of the high-fidelity physical data gets smaller, the benefit of using MFA becomes obvious, due to MFA being able to borrow strength from the simulation responses.

As the high-fidelity data points become fewer, the difference between MFA and SFA once again diminishes. We believe that there are two reasons behind this behavior. The first reason is common to all MFA problems. When the high-fidelity data points are sparse, the dominance due to large amount of low-fidelity data is much more pronounced and the benefit of using a combining with MFA becomes compromised. This reason alone, however, cannot explain the trend shown in Fig. 4, in which for three or four high-fidelity data points, MFA produces a slight improvement over SFA. Previous studies in the literature concerning MFA w/o LA have reported a somewhat different insight: when the number of high-fidelity data points becomes very small, the benefit of using MFA, albeit compromised, remains significant; for an example, please see table VII of Xia (2008, p. 90).

That is why we believe that for the problems of MFA with LA, the second reason is more important. The existence of latent variables forces us to include another layer of estimation, which is to use the multi-fidelity data to find out the linkage function between the observable and unobservable variables. The quality of this estimation action suffers when the number of high-fidelity data points is too few. In turn, a poorly estimated linkage function does not result in making the combined predictions better than that from SFA.

This analysis tells us that an MFA with LA analysis will be effective only for the right range of the number of high-fidelity data points. The lower bound of this range depends on the number of data points that can provide a quality estimation of the linkage function, and the upper bound is decided by the number of data points that can make SFA self-sufficient. Our experience indicates that there is generally a considerable gap between the two bounds for practical problems, thereby rendering the MFA with LA approach a useful methodology.

4.3. Choices of linkage functions

We compared different linkage functions g that could potentially be used in the proposed method. Our aim was to investigate the effect of the functional form specified for linking the two sets of data sources and substantiate the specific choice of the linkage function made in the previous sections.

We considered two sets of alternatives. The first was a more complex class \mathcal{G} whose elements were expressed as the sum of two decreasing splines. Specifically, for the form defined in Equation (9), we let $Q = 2$, which means that each function in \mathcal{G} is the sum of two exponential func-

Table 2. Comparing different linkage functions in terms of SRMSE: the rightmost column denotes the linkage function used in Section 4.1

	SRMSE			SRMSE
	Linear	Quadratic	$Q = 2$	$Q = 1$
EXT	0.0490	0.0570	0.0898	0.0392
INT	0.0409	0.1753	0.0504	0.0383

tions. Comparing the choice between $Q = 1$ versus $Q = 2$ was intended to provide some insights into the question of whether a more complex class of functions would improve the prediction accuracy. The second set was the consideration of polynomial functions that are popularly used in curve fitting. Specially, we considered the linear and quadratic functions. Our experience with the buckypaper fabrication process indicates that using a very complex form for the linkage function does not make the final model effective because as the number of parameters to be estimated in the subsequent optimization problem increases, the efficiency of the subsequent optimization procedure deteriorates.

Table 2 compares the different linkage functions in terms of SRMSE values for both extrapolation and interpolation cases. As evident in the table, using the class \mathcal{G} with $Q = 1$, which was the linkage function chosen in Section 4.1, produces the best results, whereas using a more complex function does not appear to benefit the final prediction objective. This is not only true from the $Q = 1$ versus $Q = 2$ comparison but also from the linear versus quadratic comparison (that is, a linear function works better).

We believe that the reason the simple linkage function is favored in our problem is based on the fact that the problem has only one observable and one unobservable variable and that the two variables appear to have a rather monotonic relationship. This may not be true for other problems. We stress that the linkage function should be chosen based on the structure of a specific problem and the availability of data. One can choose other classes of functions in the case of a viable justification for the problem of interest. Also, more data points can offer the opportunity to use a linkage function that consists of more parameters and thus can handle a linkage relationships with complicated forms.

5. Conclusions

We have developed a method for predicting the Young's modulus of PVA-treated buckypaper. The new method aggregates information from physical experiments and a finite element analysis-based simulation model. Not knowing the exact values of some inputs yields a unique data structure that hinders the use of existing MFA models such as those in Kennedy and O'Hagan (2001) and Qian and Wu

(2008). We aggregated the information in the two data sets by introducing a latent variable that represents the level of effectiveness of the PVA in each sample. The latent variable in turn helps determine the functional relationship between the effectiveness and the PVA level. Solving for the linkage functional relation leads to a multi-fidelity model that allows predictions to be made at any untried levels of the PVA.

The implementation of the proposed method in the PVA-treated buckypaper fabrication process showed that it outperformed both the existing MFA w/o LA and the SFA that ignores the low-fidelity data. A closer look revealed that in problems of MFA with LA, the proposed method appears effective when the amount of high fidelity data is in the right range. Too few high-fidelity data points does not allow a good estimation of the linkage function, and too many high-fidelity data points renders the SFA self-sufficient. In between, the proposed MFA method can exploit the valuable information in the low-fidelity (simulation) data and make an overall better prediction.

The proposed method can certainly be improved in several aspects. In particular, we believe that one critical line of research to pursue is in regard of the relation between unobserved and latent variables that we modeled through Equation (11). An alternative approach would be to utilize an EM algorithm (Dempster *et al.*, 1977) to impute the unobserved variables. Of course, this requires making assumptions on the distribution of unobserved input variables. Furthermore, one needs to express the optimization problem (1) in terms of likelihood maximization. This does not appear to be straightforward.

In terms of practicality, it would be useful to develop guidelines to evaluate the similarity between the simulation outputs and the physical responses, which should be used to justify the action of integrating the simulation and physical responses. Not much has yet been published on a specific guideline or quantitative measure. One work that alludes to this aspect is Xiong *et al.* (2013), which sets a threshold on testing the cross-validation error for continuation in a sequential design. Using this cross-validation measure does shed light on how a multi-fidelity model improves the predictive outcome, but one would still not know whether a multi-fidelity design is worth it or not until the cross-validation error is computed (which has to be done after the multi-fidelity model is established). We believe that this is an unsettled issue needing attention from the academic community.

Funding

The authors would like to acknowledge the generous support from their sponsors. Ding and Pourhabib are partially supported by NSF under grant no. CMMI-1000088; Ding and Huang are partially supported by AFOSR DDDAS program under grant no. FA9550-13-1-0075 and King Ab-

dullah University of Science and Technology award KUS-CI-016-04; Huang is partially supported by NSF under grant no. DMS-1208952.

References

- Bayarri, M.J., Berger, J.O., Paulo, R., Sacks, J., Cafeo, J.A., Cavendish, J., Lin, C.-H. and Tu, J. (2007) A framework for validation of computer models. *Technometrics*, **49**(2), 138–154.
- Dempster, A.P., Laird, N.M. and Rubin, D.B. (1977) Maximum likelihood from incomplete data via the EM algorithm. *Journal of the Royal Statistical Society, Series B*, **39**(1), 1–38.
- Draguljć, D., Dean, A.M. and Santner, T.J. (2012) Non-collapsing space-filling designs for bounded nonrectangular regions. *Technometrics*, **54**(2), 169–178.
- Goldstein, M. and Rougier, J. (2006) Bayes linear calibrated prediction for complex systems. *Journal of the American Statistical Association*, **101**(475), 1132–1143.
- Goldstein, M. and Rougier, J. (2009) Reified bayesian modelling and inference for physical systems. *Journal of Statistical Planning and Inference*, **139**(3), 1221–1239.
- Han, G., Santner, T.J. and Rawlinson, J.J. (2009) Simultaneous determination of tuning and calibration parameters for computer experiments. *Technometrics*, **51**(4), 464–474.
- Hastie, T., Tibshirani, R. and Friedman, J. (2001) *Elements of Statistical Learning: Data Mining, Inference and Prediction*. Springer, New York.
- Higdon, D., Kennedy, M., Cavendish, J.C., Cafeo, J.A. and Ryne, R.D. (2004) Combining field data and computer simulations for calibration and prediction. *SIAM Journal on Scientific Computing*, **26**(2), 448–466.
- Iijima, S. (1991) Helical microtubules of graphitic carbon. *Nature*, **354**(6348), 56–58.
- Johnson, M., Moore, L. and Ylvisaker, D. (1990) Minimax and maximin distance designs. *Journal of Statistical Planning and Inference*, **26**(2), 131–148.
- Joseph, V.R. and Melkote, S.N. (2009) Statistical adjustments to engineering models. *Journal of Quality Technology*, **41**(4), 362–375.
- Kennedy, M.C. and O'Hagan, A. (2000) Predicting the output from a complex computer code when fast approximations are available. *Biometrika*, **87**(1), 1–13.
- Kennedy, M.C. and O'Hagan, A. (2001) Bayesian calibration of computer models. *Journal of the Royal Statistical Society: Series B (Statistical Methodology)*, **63**(3), 425–464.
- Qian, P.Z. (2012) Sliced Latin hypercube designs. *Journal of the American Statistical Association*, **107**(497), 393–399.
- Qian, P.Z. and Wu, C.J. (2009) Sliced space-filling designs. *Biometrika*, **96**(4), 945–956.
- Qian, P.Z.G. and Wu, C.F.J. (2008) Bayesian hierarchical modeling for integrating low-accuracy and high-accuracy experiments. *Technometrics*, **50**(2), 192–204.
- Qian, Z., Seepersad, C.C., Joseph, V.R., Allen, J.K. and Wu, C.F.J. (2006) Building surrogate models based on detailed and approximate simulations. *Journal of Mechanical Design*, **128**(4), 668–677.
- Ramsay, J. (1998) Estimating smooth monotone functions. *Journal of the Royal Statistical Society: Series B (Statistical Methodology)*, **60**(2), 365–375.
- Rasmussen, C.E. and Williams, C.K.I. (2006) *Gaussian Processes for Machine Learning*. MIT Press, Cambridge, MA.
- Reese, C.S., Wilson, A.G., Hamada, M., Martz, H.F. and Ryan, K.J. (2004) Integrated analysis of computer and physical experiments. *Technometrics*, **46**(2), 153–164.
- Santner, T.J., Williams, B.J. and Notz, W.I. (2003) *The Design and Analysis of Computer Experiments*. Springer Verlag, New York.

- Stinstra, E., Stehouwer, P., den Hertog, D. and Vestjens, A. (2003) Constrained maximin designs for computer experiments. *Technometrics*, **45**(4), 340–346.
- Tsai, C., Zhang, C., David, J.A., Wang, B. and Liang, R. (2011) Elastic property prediction of single-walled carbon nanotube buckypaper/polymer nanocomposites: stochastic bulk response modeling. *Journal of Nanoscience and Nanotechnology*, **11**(3), 2132–2141.
- Wang, K. (2013) Statistics-enhanced multistage process models for integrated design and manufacturing of poly (vinyl alcohol) treated buckypaper, Ph.D. Thesis, Florida State University, Tallahassee, FL.
- Wang, Z., Liang, Z., Wang, B., Zhang, C. and Kramer, L. (2004) Processing and property investigation of single-walled carbon nanotube (swnt) buckypaper/epoxy resin matrix nanocomposites. *Composites Part A: Applied Science and Manufacturing*, **35**(10), 1225–1232.
- Wikle, C.K. and Berliner, L.M. (2005) Combining information across spatial scales. *Technometrics*, **47**, 80–91.
- Xia, H. (2008) Bayesian hierarchical model for combining two-resolution metrology data. Ph.D. Thesis, Texas A&M University, College Station, TX.
- Xia, H., Ding, Y. and Mallick, B. (2011) Bayesian hierarchical model for combining misaligned two-resolution metrology data. *IIE Transactions*, **43**(4), 242–258.
- Xiong, S., Qian, P.Z.G. and Wu, C.F.J. (2013) Sequential design and analysis of high-accuracy and low-accuracy computer codes. *Technometrics*, **55**(1), 37–46.
- Xiong, Y., Chen, W., Tsui, K.-L. and Apley, D.W. (2009) A better understanding of model updating strategies in validating engineering models. *Computer Methods in Applied Mechanics and Engineering*, **198**(15-16), 1327–1337.
- Zhang, C., Wang, K., Liang, Z. and Wang, B. (2011) Fast filtration synthesis method for buckypaper using highly concentrated carbon nanotube slurry, presented at the INFORMS Annual Meeting, Charlotte, NC, November 13-16, 2011.

Biographies

Arash Pourhabib received his B.S. in Industrial Engineering from Sharif University of Technology in 2008, and his Ph.D. from the Department of Industrial and Systems Engineering at Texas A&M University in 2014. He is currently an Assistant Professor at the School of Industrial Engineering and Management at Oklahoma State University. His research interests are in the areas of system informatics and control and statistical machine learning. He is a member of INFORMS and IIE.

Jianhua Huang received his B.S. degree in 1989 and M.S. degree in 1992, both in Probability and Statistics, from Beijing University, China, and his Ph.D. in Statistics from the University of California, Berkeley, in 1997. He is currently a Professor of Statistics at Texas A&M University. His research interests include computational statistics, semi- and non-parametric statistical methods, statistical machine learning, and applied statistics. He is a fellow of ASA and IMS.

Dr. Kan Wang is a Post-Doctoral Researcher in the Georgia Tech Manufacturing Institute and H. Milton Stewart School of Industrial and Systems Engineering at the Georgia Institute of Technology. He received his Ph.D. (2013) in Industrial & Manufacturing Engineering from the Florida State University. After his graduation, he worked as a major

researcher in several projects sponsored by various organizations and industrial companies including National Science Foundation, Air Force Office of Scientific Research, Veterans Affairs, ATK, and Genesis Engineering Solutions. His research fields include computational modeling and simulation of manufacturing processes, additive manufacturing, and nanomaterials and nanomanufacturing.

Chuck Zhang is a Professor in the H. Milton Stewart School of Industrial and Systems Engineering at the Georgia Institute of Technology. He is also an affiliated faculty member of the Georgia Tech Manufacturing Institute. He received his Ph.D. (1993) in Industrial Engineering from the University of Iowa and was on the faculty of the Industrial & Manufacturing Engineering Department at Florida A&M University–Florida State University College of Engineering prior to joining Georgia Tech. His research interests include advanced composites/nanocomposite materials manufacturing, integrated computational materials engineering, additive manufacturing/printed electronics, and geometric tolerancing and metrology. His research projects have been sponsored by a number of organizations including the Air Force Office of Scientific Research, the Army Research Laboratory, the National Institute of Standards and Technology, the National Science Foundation, the Office of Naval Research, the Society of Manufacturing Engineers, and Veterans Affairs, as well as industrial companies such as ATK, Cummins, General Dynamics, Lockheed Martin, and Siemens Power Generation. He has published over 140 refereed journal articles and 180 conference papers. He also holds 15 U.S. patents.

Dr. Ben Wang is the Chief Manufacturing Officer of the Georgia Institute of Technology and Executive Director of the Georgia Tech Manufacturing Institute. He is a Professor and Gwaltney Chair in Manufacturing Systems in the School of Industrial and Systems Engineering and Professor in the School of Materials Science and Engineering. He serves on the National Materials and Manufacturing Board, National Research Council of the National Academies. He is a Fellow of the Institute of Industrial Engineers, Society of Manufacturing Engineers, and Society for the Advancement of Materials and Process Engineering. He has published more than 220 papers in refereed journals and is a co-inventor on 25 patents or patent applications. With a primary research interest in applying emerging technologies to improve manufacturing competitiveness, he specializes in process development for affordable composite materials and is widely acknowledged as a pioneer in the growing field of nano-materials. Currently, he focuses his research on high-performance and affordable composites, which is already changing product innovations worldwide. His attention to applications of the integrated product-process design approach toward substituting metal structures with low-cost, high-performance composite materials is unique among researchers in these difficult, yet most promising, investigations.

Yu Ding received a B.S. in Precision Engineering from the University of Science and Technology of China in 1993; an M.S. in Precision Instruments from Tsinghua University, China, in 1996; an M.S. in Mechanical Engineering from Pennsylvania State University in 1998; and a Ph.D. in Mechanical Engineering from the University of Michigan in 2001. He is currently the Mike and Sugar Barnes Professor of Industrial and Systems Engineering and Professor of Electrical and Computer Engineering at Texas A&M University. His research interests are in the area of systems informatics and quality and reliability engineering. He currently serves as a Department Editor of *IIE Transactions*. He is a member of IIE, a senior member of IEEE, and a member of INFORMS, ASQ, and ASME.